ARMY RESEARCH LABORATORY

Angle of Arrival Estimation for Saturated Acoustic Signals

by Ananth V. Sridhar, Brandon K. Au, and Geoffery H. Goldman

ARL-TR-6385 **March 2013**

NOTICES

Disclaimers

The findings in this report are not to be construed as an official Department of the Army position unless so designated by other authorized documents.

Citation of manufacturer's or trade names does not constitute an official endorsement or approval of the use thereof.

Destroy this report when it is no longer needed. Do not return it to the originator.

Army Research Laboratory
Adelphi, MD 20783-1197

ARL-TR-6385 **March 2013**

Angle of Arrival Estimation for Saturated Acoustic Signals

Ananth V. Sridhar, Brandon K. Au, and Geoffery H. Goldman
Sensors and Electron Devices Directorate, ARL

REPORT DOCUMENTATION PAGE

Form Approved
OMB No. 0704-0188

1. REPORT DATE *(DD-MM-YYYY)*	2. REPORT TYPE	3. DATES COVERED (From - To)
March 2013	Final	

4. TITLE AND SUBTITLE
Angle of Arrival Estimation for Saturated Acoustic Signals

5a. CONTRACT NUMBER

5b. GRANT NUMBER

5c. PROGRAM ELEMENT NUMBER

6. AUTHOR(S)
Ananth V. Sridhar, Brandon K. Au, and Geoffery H. Goldman

5d. PROJECT NUMBER

5e. TASK NUMBER

5f. WORK UNIT NUMBER

7. PERFORMING ORGANIZATION NAME(S) AND ADDRESS(ES)
U.S. Army Research Laboratory
ATTN: RDRL-SES-P
2800 Powder Mill Road
Adelphi, MD 20783-1197

8. PERFORMING ORGANIZATION REPORT NUMBER
ARL-TR-6385

9. SPONSORING/MONITORING AGENCY NAME(S) AND ADDRESS(ES)

10. SPONSOR/MONITOR'S ACRONYM(S)

11. SPONSOR/MONITOR'S REPORT NUMBER(S)

12. DISTRIBUTION/AVAILABILITY STATEMENT
Approved for public release; distribution unlimited.

13. SUPPLEMENTARY NOTES

14. ABSTRACT
The U.S. Army Research Laboratory (ARL) has developed a tetrahedral microphone array system for acoustic-based target detection and localization. Time-domain data can be used to obtain differential time of arrival (DTOA) and angle of arrival (AOA) estimates. Use of multiple arrays allows for triangulation. However, limitations in acoustic detection hardware, such as microphone and analog-to-digital converter (ADC) dynamic range can produce inaccurate results for large amplitude signals. Saturation can occur due to close proximity to a large transient event, which can render target localization difficult with many standard algorithms. Our goal is to develop an algorithm to detect transient events that saturate an acoustic system and estimate the AOA. This is done in three parts—detection, window selection, and AOA estimation. We have achieved a 100% detection rates with no false alarms for an ARL tetrahedral microphone array located approximately 60 m from the launch position of a large-caliber, indirect fire weapons system. After outlier removal, the average absolute deviations of the AOA errors were within 5° of the true angle.

15. SUBJECT TERMS
Acoustic, detection, saturation, microphone, least squares, transient event

16. SECURITY CLASSIFICATION OF:			17. LIMITATION OF ABSTRACT	18. NUMBER OF PAGES	19a. NAME OF RESPONSIBLE PERSON
a. REPORT	b. ABSTRACT	c. THIS PAGE			Ananth V. Sridhar
Unclassified	Unclassified	Unclassified	UU	22	19b. TELEPHONE NUMBER (*Include area code*) (301) 394-2251

Contents

List of Figures

List of Tables

Acknowledgments

We wish to acknowledge the mentorship and guidance of Geoffrey Goldman throughout this project. In addition, we would like to thank Kirk Alberts, Duong Tran-Luu, and Leng Sim for their advice and support.

INTENTIONALLY LEFT BLANK.

1. Introduction

The U.S. Army is interested in acoustic detection systems for identification and localization of large transient events. Advantages of using acoustic systems include low maintenance, omnidirectional sensing capabilities, and minimal data storage requirements. As such, these systems provide a low-cost, broad-spectrum solution to providing a method of determining target positions in the field (Goldman, 2011). Use of a tetrahedral microphone array system allows for target localization based on triangulation.

In 2011, the U.S. Army Research Laboratory (ARL) conducted research on transient event localization using microphone array systems. Testing occurred at the Blossom Point Research Facility, with four tetrahedral arrays. Over three days, large-caliber weapons systems were fired from a fixed location, as indicated in figure 1. Acoustic data were loaded into a buffer and recorded at a fixed time interval. Data were converted using a 24-bit analog-to-digital converter (ADC) (Tenney, 2004). The data were sampled at an average frequency of 9765 Hz.

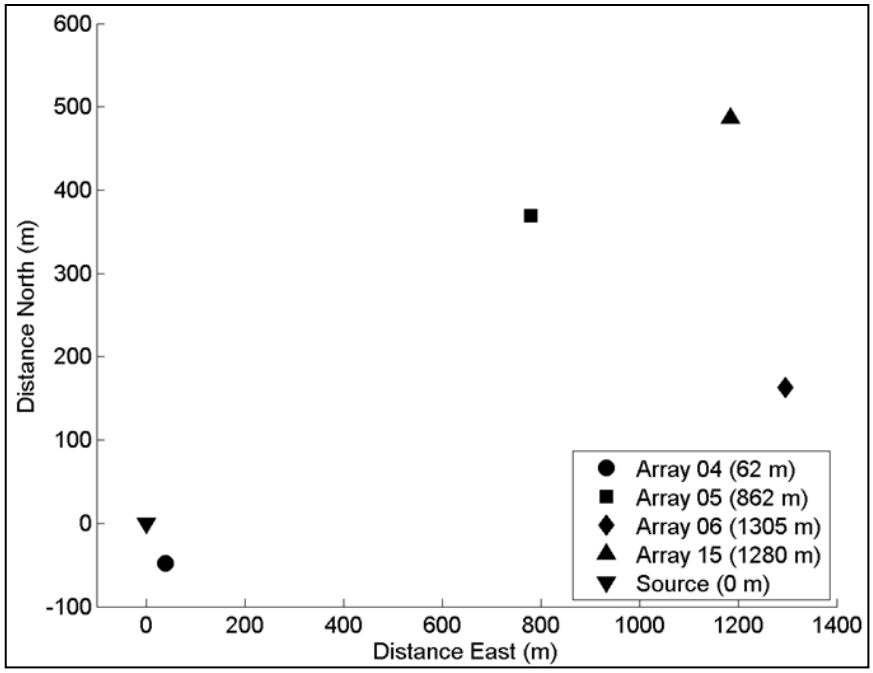

Figure 1. Tetrahedral microphone array positions during the Blossom Point experiment. The numbers in parentheses indicate distance from source.

Differential time of arrival (DTOA) and angle of arrival (AOA) estimation algorithms must function over a large dynamic range. Standard signal processing algorithms execute when a signal has crossed a pre-defined threshold on multiple channels. However, close proximity to an

acoustic source can result in signal saturation, where data reach a hardware limited rail, either due to microphone or amplifier saturation. This can result in incorrect estimates for many standard algorithms. Presented in this report is a solution to calculating AOA estimates for events that saturate the system. This is accomplished with multiple algorithms for detection, data association, and AOA estimation. Data from Array 04 of the Blossom Point experiment are used for analysis.

2. Experiment/Calculations

2.1 Detection

To develop suitable detection algorithms, data were analyzed to qualify saturation events. Hardware restrictions on the ADC resulted in a dynamic range of –6.666 to 6.666 V. As such, $|V| = 6.666$ was defined as a requirement for single channel saturation. To accurately reflect field conditions, algorithms had no user input supplying approximate event time. Based on visual inspection of the waveforms, three detection algorithms were developed.

The first and second detection algorithms used a rail identifier method to determine the time of a saturation event. The algorithms analyzed four channels of time-domain data, returning timestamps of instances where the signal reached its threshold value. The first sought to identify instances where the signal reached a lower rail voltage of $V = -6.666$, while the second algorithm identified $V = +6.666$. These lower- and upper-rail algorithms trigger for a sample that meets its requirement and then establish a 1-s suspension interval to account for hardware recovery time. This prevents multiple detections for the same saturation event. A detection is recorded only if the trigger voltage is met on all four channels. The third approach to detection relied on a large change in signal amplitude over a short sampling interval. The algorithm required a change of 12 V in 0.5 ms. As with the rail detection algorithms, a 1-s suspension and four-channel detection requirement was used to prevent multiple detections from occurring for the same event.

Figure 2 represents detection algorithm performance over a three-day period with 79 large transient events. The data show that the lower-rail approach yielded a 100% detection rate, picking up 85 detections. The extra samples are attributable to airburst and surface impact events that also saturated Array 04, and are not considered to be false alarms. The upper-rail detection algorithm showed significantly poorer performance. Inspection of time-domain signals showed that raw data did not always reach the upper rail, resulting in missed detections. This is shown in figure 3, where there is a peak of 4.8 V, with signal saturation on the lower rail at around 0.008 s. Rapid change detection, operating on signal amplitude change, showed the worst

performance. Highly variable waveforms ahead of saturation failed to produce sufficient signal changes. Comparative performance of the three algorithms indicated that the lower-rail approach was superior for detection.

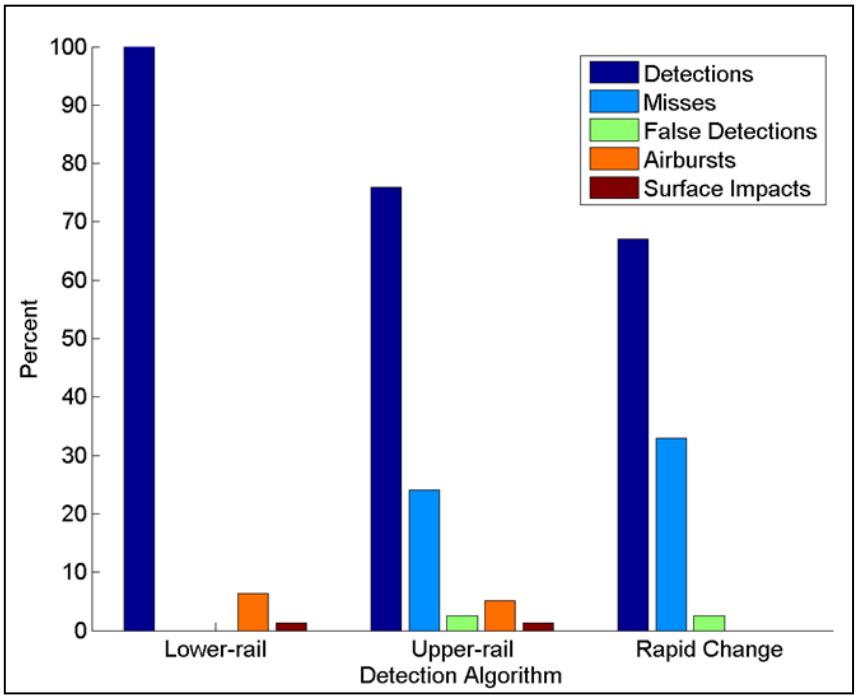

Figure 2. Performance of three detection algorithms.

2.2 DTOA Computation

Once an event is detected, the program estimates the DTOA at each microphone in the array. There are three approaches to computing these DTOAs. The first approach is to cross-correlate the signal before saturation. The second and third approaches use the saturation time and polynomial interpolation algorithms, respectively.

To find DTOAs with cross-correlation, an appropriate data window must be selected. Window selection is accomplished with a crawler algorithm. Starting 200 ms before a channel's saturation time, the algorithm identifies the time at which the signal exceeds a program-specified voltage (0.5 V). This is the window start time. The window ends 0.2 ms (two samples) before a channel's saturation. A constant window size is used for all the channels. Figure 3 shows an example of a chosen window. These constraints attempted to optimize the window for a high signal-to-noise ratio (SNR). The result is six DTOA estimates calculated using four channels of data collected on the tetrahedral array.

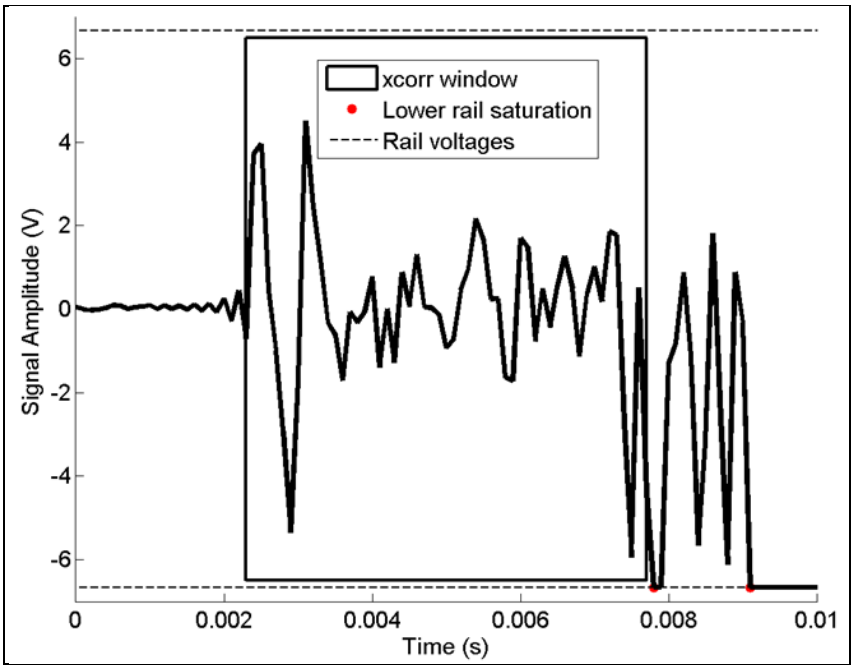

Figure 3. One channel of signal saturation.

The second approach to estimate the DTOA uses the differences between channel saturation times. However, this solution is prone to mistiming due to the variability in sustained saturation. Figure 3 indicates one such instance, where channel 1 of Array 04 saturates briefly (first red point), oscillates, and then saturates for a prolonged period (second red point). As a third approach, the DTOA is also estimated using a polynomial interpolation algorithm. Similar to the cross-correlation algorithm, a crawler starts 200 ms before saturation and identifies the first sample that exceeds a threshold voltage set at 4 V. Then, it considers two additional samples, one before and one after the identified point. The discrete nature of the data results in an approximate solution for the time at which the threshold voltage is reached. Solving a linear system with these three points yields a quadratic equation, which can be used to produce more accurate estimates. However, this method does not guarantee that the signal will exceed the threshold value before saturating. As such, the polynomial interpolation-based DTOAs estimates are not computed for all the saturation events.

2.3 AOA Estimation

The AOA from Array 04 was estimated using a least squares (LS) approach. Employing a far-field approximation, the DTOA of a signal from the source to Array 04 is given by

$$\Delta t_{i,j} = \frac{\vec{a}^T \cdot (\vec{P_i} - \vec{P_j})}{c} \quad (1)$$

where $\overrightarrow{P_i}$ and $\overrightarrow{P_j}$ represent the positions of the i^{th} and j^{th} microphones (shown in figure 4), c represents signal propagation speed ($340\,\frac{\mathrm{m}}{\mathrm{s}}$), $\Delta t_{i,j}$ represents the estimated time difference between microphones i and j, and $\vec{a}$ represents the direction of arrival (DOA) vector (Goldman, 2011). The DOA is estimated using a LS approach,

$$\epsilon = \sum_{i=1}^{4}\sum_{j=i+1}^{4}\left(\widehat{\Delta t_{i,j}} - \Delta t_{i,j}\right)^2 = \sum_{i=1}^{4}\sum_{j=i+1}^{4}\left(\widehat{\Delta t_{i,j}} - \frac{\vec{a}^T\cdot\left(\overrightarrow{P_i}-\overrightarrow{P_j}\right)}{c}\right)^2 \quad (2)$$

where $\widehat{t_{i,j}}$ represents the estimated DTOAs calculated from cross-correlation, saturation time delays, or polynomial interpolation.

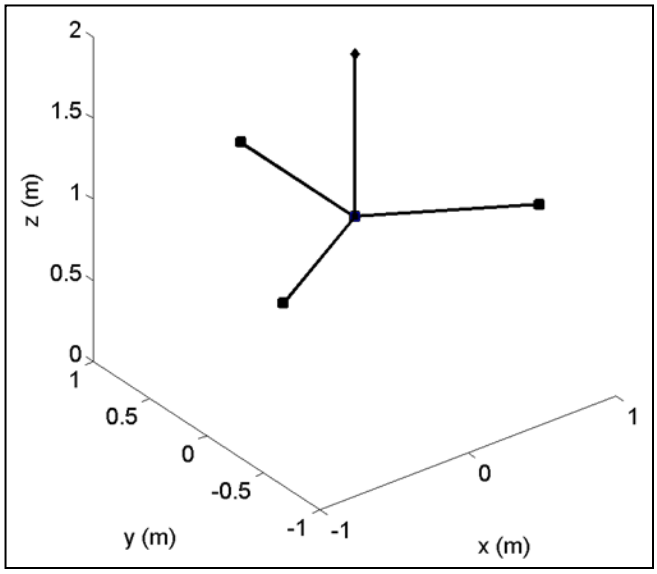

Figure 4. Configuration of tetrahedral microphone array. Squares indicate the microphone positions.

3. Results and Discussion

AOA results are presented for the LS approach using inputs from three DTOA estimations. A lower-rail detection algorithm was used to estimate the TOA. DTOA were estimated using algorithms based on cross-correlation, saturation times, and polynomial interpolation. Six DTOAs obtained from each algorithm were processed to obtain AOA by minimizing the error function (*2*). The resulting AOA estimates for the three approaches are shown in figures 5, 6, and 7. For visualization purposes, displayed data have been restricted between $[100°, 160°]$.

Figure 8 shows the absolute error of AOA outputs on a logarithmic scale calculated using $20 * \log_{10}(|\theta - \theta_{true}|)$. To preserve the sign of the error, results for which $\theta - \theta_{true} > 0$ are shown

in the upper row, while results for which $\theta - \theta_{true} < 0$ is shown in the lower row. The *x*-axis scales are given in both decibels and degrees. The graph shows that a majority of error was between 1° and 10° of θ_{true}. Error greater than 10° is present in methods 1 and 2 for detections, and in all three DTOA approaches for airburst and surface impact events.

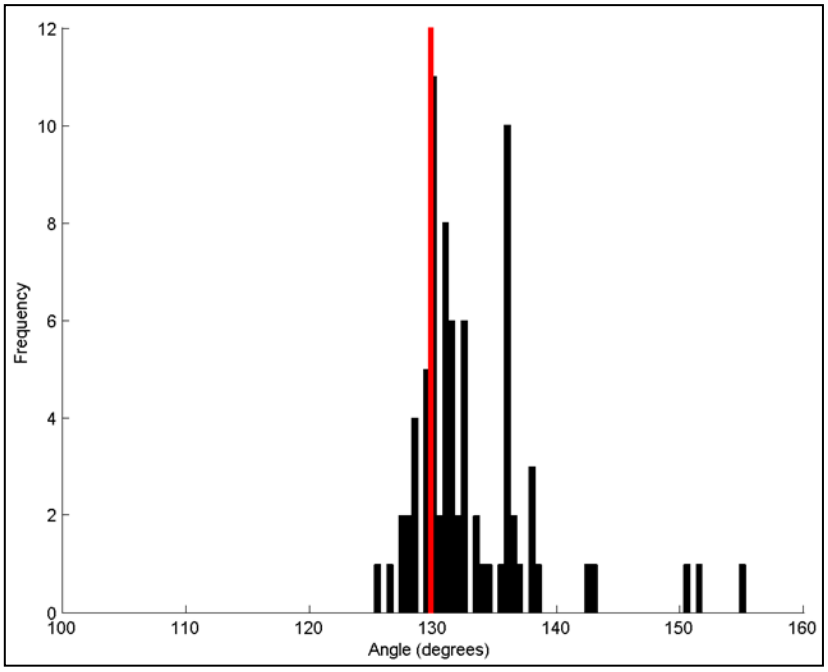

Figure 5. Estimated AOAs from a cross-correlation DTOA estimation. The red line indicates true source angle.

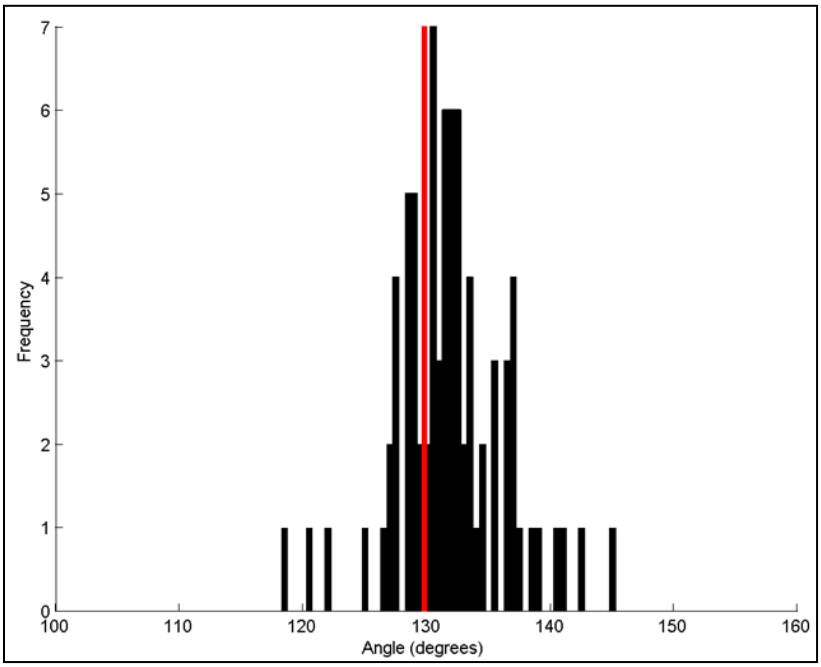

Figure 6. Estimated AOAs from a saturation time delay DTOA estimation. The red line indicates true source angle.

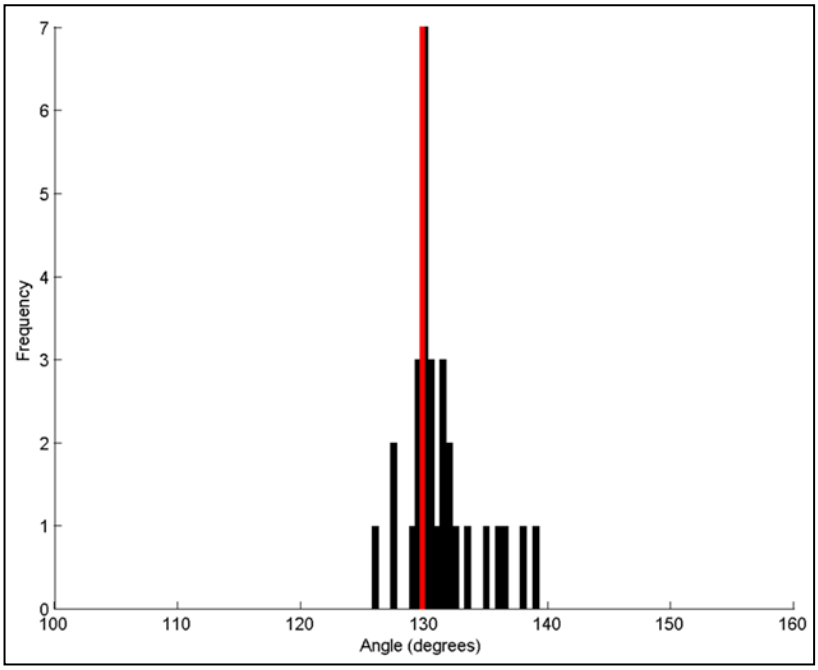

Figure 7. Estimated AOAs from polynomial interpolation DTOA estimation. The red line indicates true source angle.

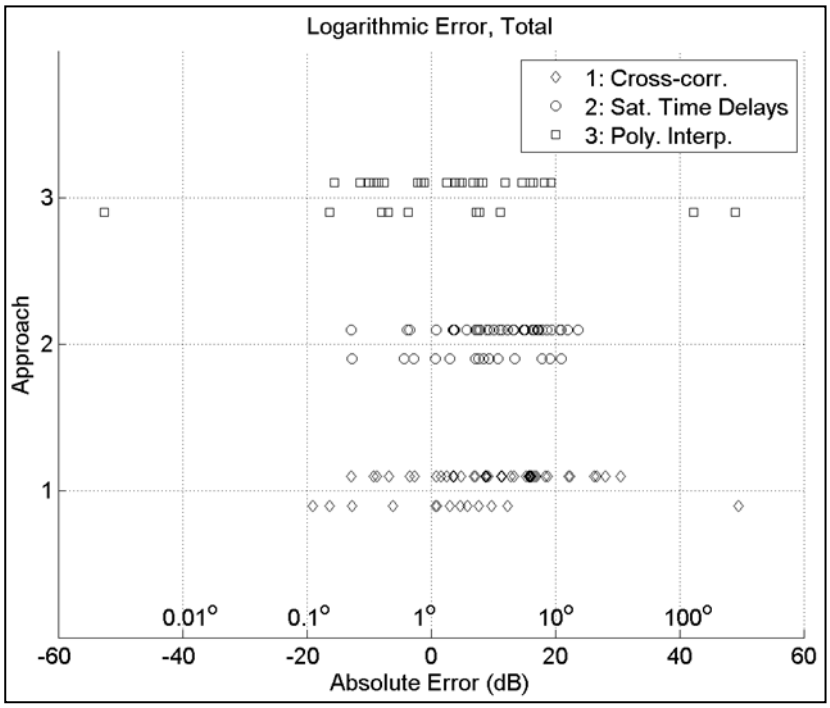

Figure 8. Positive and negative DTOA estimation errors. Positive errors are above the negative errors are below each approach.

Table 1 displays statistics for each DTOA estimation method. Cross-correlation and saturation time delay statistics are given for all launch detections. Table 2 gives values for all DTOA approaches, considering only those detections that were processed by polynomial interpolation. Measures of central tendency (mean, median) were computed with respect to the ground-truth angle, $\theta_{true} = 129.97°$ (Van Trees, 2002; Sheshkin, 1997). Statistics were computed for two subsets of a DTOA calculation method—the entire data set (ALL) and interquartile range (IQR), which eliminated the lower and upper 25% of AOAs. The IQR was chosen as a subset to exclude AOAs resulting from airburst, surface impact, or strong wind effects.

A comparison between cross-correlation and saturation time delay is shown in table 1. The results indicate that the saturation time delays algorithm results in more precise AOA estimates. This is supported by the small standard deviation of the saturation time delay data versus that of cross-correlation. Comparisons of standard deviations between the approaches for IQR values yield comparable results, indicating that the wider dispersion in cross-correlation AOA is due to only a few outliers. Figure 8 indicates that there is an even distribution of error present for saturation time delays, whereas cross-correlation is positively biased. A comparison of the AOA algorithms shown in table 2 indicate that polynomial interpolation was subject to the same spread as cross-correlation, due to a small number of outliers in its processed AOA data. However, its median absolute deviation had the smallest time delay errors.

Table 1. Metrics for AOA estimation, full sample range.

Measure	DTOA estimation method	ALL (°)	IQR (°)
Standard Deviation: $\boldsymbol{\sigma}$	Cross-correlation	34.42	1.76
	Saturation Time Delays	4.46	1.26
Median Absolute Deviation: $\widetilde{\left|\boldsymbol{\theta}-\widetilde{\boldsymbol{\theta}}\right|}$	Cross-correlation	2.03	1.18
	Saturation Time Delays	2.18	0.90
Average Absolute Deviation: $\overline{\left|\boldsymbol{\theta}-\overline{\boldsymbol{\theta}}\right|}$	Cross-correlation	8.03	1.41
	Saturation Time Delays	3.25	1.08
RMS Deviation: $(\boldsymbol{\theta}-\boldsymbol{\theta}_{\boldsymbol{rms}})_{\boldsymbol{rms}}$	Cross-correlation	34.49	1.74
	Saturation Time Delays	4.43	1.25
Difference between Median and True: $\widetilde{\boldsymbol{\theta}}-\boldsymbol{\theta}_{\boldsymbol{true}}$	Cross-correlation	1.54	1.54
	Saturation Time Delays	1.56	1.55
Difference between Mean and True: $\overline{\boldsymbol{\theta}}-\boldsymbol{\theta}_{\boldsymbol{true}}$	Cross-correlation	−0.12	2.10
	Saturation Time Delays	2.08	1.71
Difference between RMS and True: $\boldsymbol{\theta}_{\boldsymbol{rms}}-\boldsymbol{\theta}_{\boldsymbol{true}}$	Cross-correlation	4.31	2.11
	Saturation Time Delays	2.16	1.72

Table 2. Metrics for AOA estimation, reduced polynomial interpolation range.

Measure	DTOA estimation method	ALL (°)	IQR (°)
Standard Deviation: $\boldsymbol{\sigma}$	Cross-correlation	53.14	0.62
	Saturation Time Delays	3.09	0.93
	Polynomial Interpolation	54.58	0.71
Median Absolute Deviation: $\widetilde{\left|\boldsymbol{\theta}-\widetilde{\boldsymbol{\theta}}\right|}$	Cross-correlation	1.02	0.44
	Saturation Time Delays	1.72	0.67
	Polynomial Interpolation	1.13	0.38
Average Absolute Deviation: $\overline{\left|\boldsymbol{\theta}-\overline{\boldsymbol{\theta}}\right|}$	Cross-correlation	18.12	0.53
	Saturation Time Delays	2.21	0.79
	Polynomial Interpolation	24.29	0.58
RMS Deviation: $(\boldsymbol{\theta}-\boldsymbol{\theta}_{\boldsymbol{rms}})_{\boldsymbol{rms}}$	Cross-correlation	53.39	0.60
	Saturation Time Delays	3.04	0.90
	Polynomial Interpolation	54.96	0.69
Difference between Median and True: $\widetilde{\boldsymbol{\theta}}-\boldsymbol{\theta}_{\boldsymbol{true}}$	Cross-correlation	0.57	0.57
	Saturation Time Delays	1.32	1.32
	Polynomial Interpolation	0.60	0.60
Difference between Mean and True: $\overline{\boldsymbol{\theta}}-\boldsymbol{\theta}_{\boldsymbol{true}}$	Cross-correlation	−7.38	0.69
	Saturation Time Delays	1.33	1.44
	Polynomial Interpolation	−11.38	0.80
Difference between RMS and True: $\boldsymbol{\theta}_{\boldsymbol{rms}}-\boldsymbol{\theta}_{\boldsymbol{true}}$	Cross-correlation	3.33	0.67
	Saturation Time Delays	1.36	1.44
	Polynomial Interpolation	0.24	0.80

4. Conclusions

Techniques were developed to detect large transient events and estimate the DTOA and AOA across a tetrahedral array. Three algorithms were developed and tested to estimate the DTOA, and a LS approach was employed to estimate AOA. A lower-rail detection algorithm recorded TOAs of saturation events and, if present across multiple channels, executed three DTOA algorithms. DTOA was calculated based on cross-correlation of four channels ahead of saturation time, differences between channel saturation times, and differences between signal threshold times. AOA estimation used a far-field approximation, seeking to minimize a sum of squared error cost function.

Data were analyzed using three DTOA algorithms. The cross-correlation algorithm and saturation time delays algorithm had 100% probability of detection with no false alarms. However, the polynomial interpolation algorithm only detected 40% of the events. Although it had a lower detection probability, the interpolation algorithm yielded the most accurate AOA estimate. The algorithm based on saturation time delay had the best overall performance.

5. References

Goldman, G. H.; Tran-Luu D. *Microphone Calibration for ARL's Unattended Transient Acoustic MASINT System*; ARL-TR-4711; U.S. Army Research Laboratory: Adelphi, MD, 2009. [SECRET]

Goldman, G.; Reiff, C. Localization Using Ground- and Air-based Acoustic Arrays. *SPIE*, 2011.

Oppenheim, A. V.; Willsky, A. S. *Signals and Systems*; USA: Prentice Hall, 1983.

Papoulis, A.; Pillai, S. *Probability, Random Variables, and Stochastic Processes*; McGraw-Hill, 2002.

Sheshkin, D. J. *Handbook of Parametric and Nonparametric Statistical Procedures*. Boca Raton, FL: CRC Press, 1997.

Tenney, S.; Mays, B.; Hillis, D.; Tran-Luu, D.; Houser, J.; Reiff, C. Acoustic Mortar Localization System – Results from OIF. *24th Army Science Conference*, Orlando, FL, December 2004.

Van Trees, H. L. *Optimum Array Processing*; New York, NY: John Wiley & Sons, 2002.

List of Symbols, Abbreviations, and Acronyms

ADC	analog-to-digital converter
ALL	complete data set
AOA	angle of arrival
ARL	U.S. Army Research Laboratory
DOA	direction of arrival
DTOA	differential time of arrival
IQR	interquartile range
LS	least squares
SNR	signal to noise ratio
TOA	time of arrival
$\tilde{x}$	median of x
$\boldsymbol{\theta_{true}}$	true angle of 129.79°
θ	calculated angles
σ	standard deviation

NO. OF COPIES	ORGANIZATION
1 ELEC	ADMNSTR DEFNS TECHL INFO CTR ATTN DTIC OCP 8725 JOHN J KINGMAN RD STE 0944 FT BELVOIR VA 22060-6218
4 PDFS	US ARMY ARDEC FUZE PRECISION ARMAMENT TECHNOLOGY DIV ATTN A MORCOS ATTN H VANPELT ATTN J CHANG ATTN S DESAI
6 PDFS	US ARMY RSRCH LAB ATTN IMAL HRA MAIL & RECORDS MGMT ATTN RDRL CIO LL TECHL LIB ATTN RDRL SES P G GOLDMAN ATTN RDRL SES P M SCANLON ATTN RDRL SES S G WILLIAMS ATTN RDRL SES S R HOLBEN

INTENTIONALLY LEFT BLANK.